Block Transmission over Multi-Scale Multi-Lag Wireless Channels

Geert Leus*, Tao Xu*, and Urbashi Mitra†

* Faculty of Electrical Engineering, Mathematics and Computer Science
Delft University of Technology, Delft, the Netherlands
{g.j.t.leus,t.xu}@tudelft.nl

† Ming Hsieh Department of Electrical Engineering
University of Southern California, Los Angeles, USA
ubli@usc.edu

***Abstract*—In this paper, new parametric models for wideband, time-varying channels are developed. These models seek to describe multi-scale, multi-lag channels. The new model is adapted from recently defined scale-lag canonical models, which suffer from model mismatch issues when employed with wavelet signaling. The main challenge of the scale-lag canonical models is the fact that they are predicated upon baseband signaling; whereas wavelet signaling is bandpass in nature. The new model accommodates the bandpass nature of the signaling scheme and enables the design of high-rate block transmission methods over multi-scale multi-lag wireless channels. Simulation results demonstrate the accuracy of the new channel model, and illustrate the performance of the related spectrally efficient communication scheme.**

I. Introduction

Wideband time-varying channels are of interest in a variety of wireless communication scenarios including underwater acoustic systems and wideband terrestrial radio frequency systems such as spread-spectrum or ultrawideband. Due to the nature of wideband propagation, such channels exhibit some fundamental differences relative to so-called *narrowband* channels. More specifically, in narrowband time-varying channels, the transmitted signal experiences multiple propagation paths each with a possibly distinct Doppler frequency *shift*, and thus these channels are also known as *multi-Doppler shift, multi-lag* channels. For wideband channels, on the other hand, each propagation path experiences a distinct Doppler scale, hence the term, *multi-scale, multi-lag* channel. For both types of time-varying channels, so-called *canonical* channel models have been proposed [1], [2], [3], [4], limiting the number of channel coefficients required to represent the channel.

In particular, there has been significant success in the application of canonical models to narrowband time-varying channels [1]. For wideband time-varying channels a canonical model has been proposed in [2], [3], [4], which we dub as the *scale-lag* canonical model. This model has been adopted for direct sequence spread spectrum (DSSS) communication systems [4] to develop a scale-lag RAKE receiver to collect the diversity inherent in the multi-scale multi-lag channel. In addition, this model has spurred the use of wavelet signaling due to the fact that when the wavelets are "matched" to the scale-lag model, the receiver structure is greatly simplified – the signals corresponding to different scale-lag branches of the model are orthogonal when a single wavelet pulse is transmitted. The single pulse case is examined in [3]. Multi-scale multi-lag wavelet signaling is possible as well [5], although inter-scale and inter-delay interference results. In [5], multiple receiver designs to combat such interference are provided exploiting the banded nature of the resulting interference.

We observe that prior art on wideband, time-varying channels often adopted different channel models. A single-scale model is commonly considered [6], [7], which greatly simplifies processing at the expense of not always modeling the wideband channel well. Approximation by a bank of multiple narrowband time-varying channels [8] can be considered as well, wherein each sub-channel is modeled by a multi-Doppler shift, multi-lag model. Finally, in [9], [10], [11], the channel itself is modeled by wavelet (packet) transforms. Although approached from a different viewpoint, these models can somehow be related to the existing scale-lag canonical models.

However, recent research points to the accuracy of the scale-lag canonical model for wideband time-varying channels. A challenge with direct application of the models of [2], [3], [4] is that most considered wavelets are badly matched to the scale-lag canonical model as this model is based on baseband signaling, whereas wavelet signaling is bandpass in nature. In this paper, we thus modify the scale-lag canonical model by exploiting the baseband feature of the signaling scheme. First, the discretization and smoothing in the scale domain is done as in [3]. This step actually reveals that we are dealing with a virtual time-invariant multiple-input single-output (MISO) system with as inputs different scaled versions of the original input. Hence, we can treat every branch as a time-invariant bandpass communication link, which we can bring back to baseband before we perform discretization and smoothing in the time domain. This finally leads to a new parametrization of the channel that better fits bandpass signals. Based on this model, we then also develop a high-rate signaling scheme and related receiver processing steps.

The outline of this paper is as follows. In Section II, we review the original scale-lag canonical channel model and demonstrate the wavelet signaling problem using this model. We solve this issue in Section III, where we adapt the original scale-lag canonical model. We use this model to develop a spectrally efficient signaling scheme in Sections IV and V. Simulation results and conclusions are presented in Sections VI and VII, respectively.

Notation: We use $(\cdot)^T$ for transpose, $\lceil\cdot\rceil$ for integer ceiling, and $\lfloor\cdot\rfloor$ for integer flooring. We reserve j for the imaginary unit, $\Re\{\cdot\}$ for the real part, and $\Im\{\cdot\}$ for the imaginary part.

This research has been funded in part by the following grants and organizations: NWO-STW under the VICI program (project 10382),ONR N00014-09-1-0700, NSF CNS-0722073, NSF CNS-0821750 (MRI), and the University of Southern California's Provost Office.

II. Scale-Lag Canonical Channel Model

A general multi-scale multi-lag wireless channel can be described as [12]

$$r(t) = \int_0^{\infty} \int_{-\infty}^{\infty} h(\alpha,\tau)\sqrt{\alpha}x(\alpha(t-\tau))d\tau d\alpha, \quad (1)$$

where $x(t)$ is the transmitted signal, $r(t)$ is the received signal, and $h(\alpha,\tau)$ is the wideband spreading function [12]. This model reflects the fact that the received signal $r(t)$ can be represented by a superposition of differently delayed (by τ) and scaled (by α) versions of the transmitted signal ($\sqrt{\alpha}$ is a normalization factor). Due to physical restrictions, τ and α can, without loss of generality, be limited to $\tau \in [0,\tau_{max}]$ and $\alpha \in [1,\alpha_{max}]$ by appropriately delaying and scaling the received signal. The parameters $\tau_{max} > 0$ and $\alpha_{max} - 1 > 0$ respectively represent the delay and scale spread.

Under certain circumstances, which we will highlight in the sequel, it has been shown that this model can be approximated by the following finite-dimensional discrete multi-scale multi-lag model, which we refer to as the *scale-lag canonical model* [2], [3], [4],

$$r^{\mathrm{SL}}(t) = \sum_{r=0}^{R_\star} \sum_{l=0}^{L_\star(r)} h_{r,l} a_\star^{r/2} x(a_\star^r(t - lT_\star/a_\star^r)), \quad (2)$$

where $T_\star$ is the arithmetic time resolution and $a_\star$ is the geometric scale resolution of the model. Further, the scale order $R_\star$ is given by $R_\star = \lceil \ln \alpha_{\max}/\ln a_\star \rceil$, and the delay order related to the rth scale $L_\star(r)$ is given by $L_\star(r) = \lceil a_\star^r \tau_{max}/T_\star \rceil$.

In [4], the time and scale resolutions of the canonical model are linked to the ambiguity function $\chi(\alpha,\tau) = \int x(t)\sqrt{\alpha}x(\alpha(t-\tau))dt$, which is assumed to decay in scale and time. More specifically, $T_\star$ is defined as the first zero-crossing of $\chi(1,\tau)$ whereas $a_\star$ as the first zero-crossing of $\chi(\alpha,0)$. However, we follow the approach of [3], where it is assumed that $x(t)$ has a limited bandwidth and Mellin support[1]. This leads to $T_\star = 1/W_\star$, where $W_\star$ is the bandwidth of $x(t)$, and $a_\star = e^{1/M_\star}$, where $M_\star$ is the Mellin support of $x(t)$. Under these conditions, $h_{r,l} = h^{\mathrm{SL}}(a_\star^r, lT_\star/a_\star^r)$, where $h^{\mathrm{SL}}(\alpha,\tau)$ is the scale-lag-smoothed version of $h(\alpha,\tau)$:

$$h^{\mathrm{SL}}(\alpha,\tau) = \int_1^{\alpha_{\max}} \int_0^{\tau_{\max}} h(\alpha',\tau') \times \mathrm{sinc}\left(\frac{\ln\alpha - \ln\alpha'}{\ln a_\star}\right) \mathrm{sinc}\left(\alpha\frac{\tau-\tau'}{T_\star}\right) d\tau' d\alpha'. \quad (3)$$

The approach of [2] is related to the approach of [3]. However, in [2] the limited bandwidth and Mellin support are explicitly obtained by operators. More specifically, whereas [3] implicitly assumes bandwidth and Mellin support limitations at the transmitter, [2] assumes the frequency support is limited at the transmitter while the Mellin support is limited at the receiver, which leads to a scale-lag-smoothed version of $h(\alpha,\tau)$ that is slightly different from (3).

As proposed in [3], [5], assume we use the model (2) to develop a wavelet signaling scheme based on a unit-energy orthogonal wavelet $\psi(t)$ showing orthogonality over a time shift of T (called base time) and scale shift of a (called base scale). A set of symbols s_n is then modulated on $\psi(t)$ at a symbol rate of T as

$$x(t) = \sum_n s_n \psi(t - nT).$$

[1]The Mellin support of a signal $x(t)$ is the support of the Mellin transform of $x(t)$ which is given by $\mathcal{M}(x(t)) = X_{\mathcal{M}}(s) = \int_0^\infty 1/t^{1/2} x(t) e^{j2\pi s \ln(t/t_{\mathrm{norm}})} dt$, where t_{norm} is a normalization time.

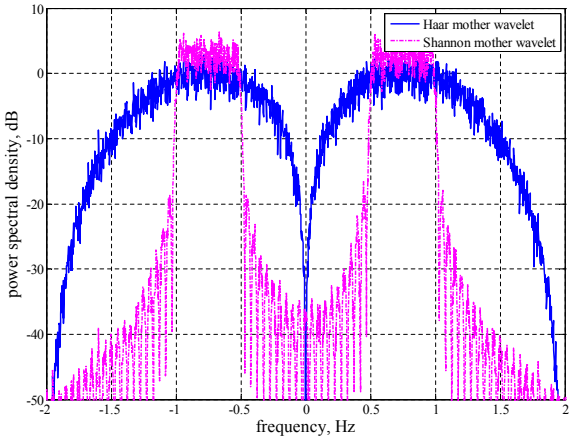

Fig. 1. Power spectral density of the Haar and Shannon mother wavelets.

A critical element of such a wavelet signaling scheme is that the base time T and base scale a of $\psi(t)$ can be properly matched to the time resolution $T_\star = 1/W_\star$ and scale resolution $a_\star = e^{1/M_\star}$ of the channel, in which case the model (2) becomes

$$r^{\mathrm{SL}}(t) = \sum_{r=0}^{R} \sum_{l=0}^{L(r)} h_{r,l} a^{r/2} x(a^r(t - lT/a^r)), \quad (4)$$

where $R = \lceil \ln \alpha_{\max}/\ln a \rceil$, $L(r) = \lceil a^r \tau_{max}/T \rceil$, and $h_{r,l}$ is defined as before but with $T_\star$ and $a_\star$ replaced by T and a, respectively. However, such a matching can only be achieved if $\psi(t)$ has a bandwidth of $1/T$ and a Mellin support of $1/\ln a$. However, most wavelets do not satisfy this property. For instance, the Haar and Shannon mother wavelets (with base time $T = 1$ and base scale $a = 2$, or *dyadic*), although having a Mellin support close to $1/\ln 2$, their bandwidth is much larger than $1/T = 1$ ($\approx$3 for Haar and 2 for Shannon), as illustrated in Figure 1.

The main reason for this problem is that wavelets are bandpass in nature in order to provide orthogonality in the scale domain. In contrast, the scale-lag canonical model has been derived assuming baseband signaling. This issue will be tackled in the next section, where we explicitly take the bandpass nature of the transmitted signal into account.

III. Proposed Channel Model

In contrast to [3], we here assume the transmitted signal $x(t)$ is a bandpass signal with carrier frequency f_c and effective bandwidth $\tilde{W}_\star$ (so $W_\star = 2f_c + \tilde{W}_\star$), and it has a Mellin support of $M_\star$. Our first step is similar to [3], and consists of discretizing the scale domain and approximating (1) by

$$r^{\mathrm{S}}(t) = \sum_{r=0}^{R_\star} \int_0^{\tau_{\max}} h_r(\tau) a_\star^{r/2} x(a_\star^r(t-\tau))d\tau, \quad (5)$$

where $a_\star = e^{1/M_\star}$, $R_\star = \lceil \ln \alpha_{\max}/\ln a_\star \rceil$, and $h_r(\tau) = h^{\mathrm{S}}(a_\star^r, \tau)$, with $h^{\mathrm{S}}(\alpha,\tau)$ the scale-smoothed version of $h(\alpha,\tau)$:

$$h^{\mathrm{S}}(\alpha,\tau) = \int_1^{\alpha_{\max}} h(\alpha',\tau)\mathrm{sinc}\left(\frac{\ln\alpha - \ln\alpha'}{\ln a_\star}\right) d\alpha'. \quad (6)$$

Observing (5), we can now interpret this system as a virtual time-invariant multiple-input single-output (MISO) system with $R_\star + 1$ branches, where the rth branch is characterized by the channel $h_r(t)$

and has as input a scaled version of the original transmitted signal, i.e., $a_\star^{r/2}x(a_\star^r t)$, which has a carrier frequency of $a_\star^r f_c$ and an effective bandwidth of $a_\star^r \tilde{W}_\star$.

We consider these branches of the virtual MISO system separately, and model the rth branch as

$$r_r^{\mathrm{S}}(t) = \int_0^{\tau_{\max}} h_r(\tau) a_\star^{r/2} x(a_\star^r(t-\tau))d\tau.$$

This looks like a traditional time-invariant bandpass communication link, and can thus also be represented by its complex baseband equivalent form as

$$\bar{r}_r^{\mathrm{S}}(t) = \int_0^{\tau_{\max}} \bar{h}_r(\tau) a_\star^{r/2} \bar{x}(a_\star^r(t-\tau))d\tau, \tag{7}$$

where $\bar{r}_r^{\mathrm{S}}(t)$, $\bar{h}_r(\tau)$, and $\bar{x}(t)$ are the complex baseband equivalent representations of $r_r^{\mathrm{S}}(t)$, $h_r(\tau)$, and $x(t)$, respectively, or in other words:

$$\begin{aligned} r_r^{\mathrm{S}}(t) &= \Re\{\bar{r}_r^{\mathrm{S}}(t)e^{j2\pi f_c a_\star^r t}\}, \\ h_r(t) &= \Re\{\bar{h}_r(t)e^{j2\pi f_c a_\star^r t}\}, \\ x(t) &= \Re\{\bar{x}(t)e^{j2\pi f_c t}\}. \end{aligned}$$

Next, we discretize the time domain. Due to the fact that $\bar{x}(t)$ has a limited bandwidth of $\tilde{W}_\star$ (or $\bar{x}(a_\star^r t)$ has a limited bandwidth of $a_\star^r \tilde{W}_\star$), we can approximate (7) as

$$\bar{r}_r^{\mathrm{SL}}(t) = \sum_{l=0}^{\tilde{L}_\star(r)} \bar{h}_{r,l} a_\star^{r/2} \bar{x}(a_\star^r(t - l\tilde{T}_\star/a_\star^r)),$$

where $\tilde{T}_\star = 1/\tilde{W}_\star$, $\tilde{L}_\star(r) = \lceil a_\star^r \tau_{max}/\tilde{T}_\star \rceil$, and $\bar{h}_{r,l} = \bar{h}_r^{\mathrm{L}}(l\tilde{T}_\star/a_\star^r)$, with $\bar{h}_r^{\mathrm{L}}(\tau)$ the lag-smoothed version of $\bar{h}_r(\tau)$:

$$\bar{h}_r^{\mathrm{L}}(\tau) = \int_0^{\tau_{\max}} \bar{h}_r(\tau') \mathrm{sinc}\left(a_\star^r \frac{\tau - \tau'}{\tilde{T}_\star}\right) d\tau'. \tag{8}$$

Finally, the adapted scale-lag canonical channel model is given by

$$\begin{aligned} r^{\mathrm{SL}}(t) &= \sum_{r=0}^{R_\star} \Re\{e^{j2\pi f_c a_\star^r t} \bar{r}_r^{\mathrm{SL}}(t)\} \\ &= \sum_{r=0}^{R_\star} \Re\left\{ e^{j2\pi f_c a_\star^r t} \sum_{l=0}^{\tilde{L}_\star(r)} \bar{h}_{r,l} a_\star^{r/2} \bar{x}(a_\star^r(t - l\tilde{T}_\star/a_\star^r)) \right\}. \end{aligned} \tag{9}$$

A schematic overview of this model is shown in Figure 2.

IV. Signaling Scheme

Suppose now that we modulate a set of symbols s_n on a carrier with frequency f_c using a unit-energy pulse shape $p(t)$ at symbol rate $\tilde{T}$. The baseband signal $\bar{x}(t)$ introduced in Section III can then be expressed as

$$\bar{x}(t) = \sum_n s_n p(t - n\tilde{T}),$$

and the related passband signal becomes

$$\begin{aligned} x(t) &= \sum_n \Re\{s_n p(t - n\tilde{T}) e^{j2\pi f_c t}\} \\ &= \sum_n \Re\{s_n\} \cos(2\pi f_c t) p(t - n\tilde{T}) \\ &\qquad - \Im\{s_n\} \sin(2\pi f_c t) p(t - n\tilde{T}). \end{aligned}$$

Further, given that $p(t)$ has a bandwidth of $\tilde{W}_\star$, we can define a scale parameter a for which the different branches of the virtual MISO system are not overlapping in the frequency domain, hence are orthogonal:

$$a = \frac{2f_c + \tilde{W}_\star}{2f_c - \tilde{W}_\star}. \tag{10}$$

Crucial to our model is now that the symbol period $\tilde{T}$ matches the time resolution $\tilde{T}_\star = 1/\tilde{W}_\star$ and that a matches $a_\star = e^{1/M_\star}$, in which case the model (9) can be written as

$$r^{\mathrm{SL}}(t) = \sum_{r=0}^{R} \Re\left\{ e^{j2\pi f_c a^r t} \sum_{l=0}^{\tilde{L}(r)} \bar{h}_{r,l} a^{r/2} \bar{x}(a^r(t - l\tilde{T}/a^r)) \right\}, \tag{11}$$

where $R = \lceil \ln \alpha_{\max} / \ln a \rceil$, $\tilde{L}(r) = \lceil a^r \tau_{max}/\tilde{T} \rceil$, and $\bar{h}_{r,l}$ is defined as before but with $\tilde{T}_\star$ and $a_\star$ replaced by $\tilde{T}$ and a, respectively.

We can then separate the different branches of the virtual MISO system by downconversion and matched filtering. More specifically, the rth branch can be obtained by downconverting the received signal with frequency $a^r f_c$ and matched filtering with $a^{r/2}p(a^r t)$. For the complex baseband equivalent representation of the rth branch, this leads to

$$\begin{aligned} \bar{y}_r^{\mathrm{SL}}(t) &= \int a^{r/2} p(a^r t') \bar{r}_r^{\mathrm{SL}}(t - t') dt' \\ &= \sum_{l=0}^{\tilde{L}(r)} \bar{h}_{r,l} \int a^{r/2} p(a^r t') \bar{x}(a^r(t - t' - l\tilde{T}/a^r)) dt' \\ &= \sum_n s_n \sum_{l=0}^{\tilde{L}(r)} \bar{h}_{r,l} \int a^r p(a^r t') p(a^r(t - t' - (l+n)\tilde{T}/a^r)) dt' \\ &= \sum_n s_n \sum_{l=0}^{\tilde{L}(r)} \bar{h}_{r,l} q_{r,l}(t - n\tilde{T}/a^r), \end{aligned}$$

where

$$q_{r,l}(t) = \int a^r p(a^r t') p(a^r(t - t' - l\tilde{T}/a^r)) dt'.$$

Sampling $\bar{y}_r^{\mathrm{SL}}(t)$ at rate $a^r/\tilde{T}$, we obtain

$$\begin{aligned} \bar{y}_{r,m} = \bar{y}_r^{\mathrm{SL}}(m\tilde{T}/a^r) &= \sum_n s_n \sum_{l=0}^{\tilde{L}(r)} \bar{h}_{r,l} q_{r,l}((m-n)\tilde{T}/a^r) \\ &= \sum_n s_n \bar{g}_{r,m-n}, \end{aligned}$$

where

$$\bar{g}_{r,n} = \sum_{l=0}^{\tilde{L}(r)} \bar{h}_{r,l} q_{r,l}(n\tilde{T}/a^r). \tag{12}$$

Hence, we obtain a standard discrete-time convolution after sampling every branch with its appropriate sampling rate, i.e., the sampling rate of the rth branch will be equal to a^r times the symbol rate $1/\tilde{T}$

The crucial question that now remains is whether we can find a waveform $p(t)$ for which $\tilde{T}$ is matched to $\tilde{T}_\star = 1/\tilde{W}_\star$ and a to $a_\star = e^{1/M_\star}$. It turns out that these matching problems can be solved by taking $p(t)$ equal to a unit-energy sinc function:

$$p(t) = \tilde{W}_\star^{1/2} \mathrm{sinc}(\tilde{W}_\star t) = 1/\tilde{T}_\star^{1/2} \mathrm{sinc}(t/\tilde{T}_\star). \tag{13}$$

First of all, a natural choice for the symbol period related to this $p(t)$ is given by $\tilde{T} = \tilde{T}_\star = 1/\tilde{W}_\star$. Further, it turns out that for this $p(t)$, the a defined in (10) satisfies $a \approx a_\star = e^{1/M_\star}$, where $M_\star$ is the Mellin support of $\cos(2\pi f_c t)p(t)$ or $\sin(2\pi f_c t)p(t)$, as indicated before.

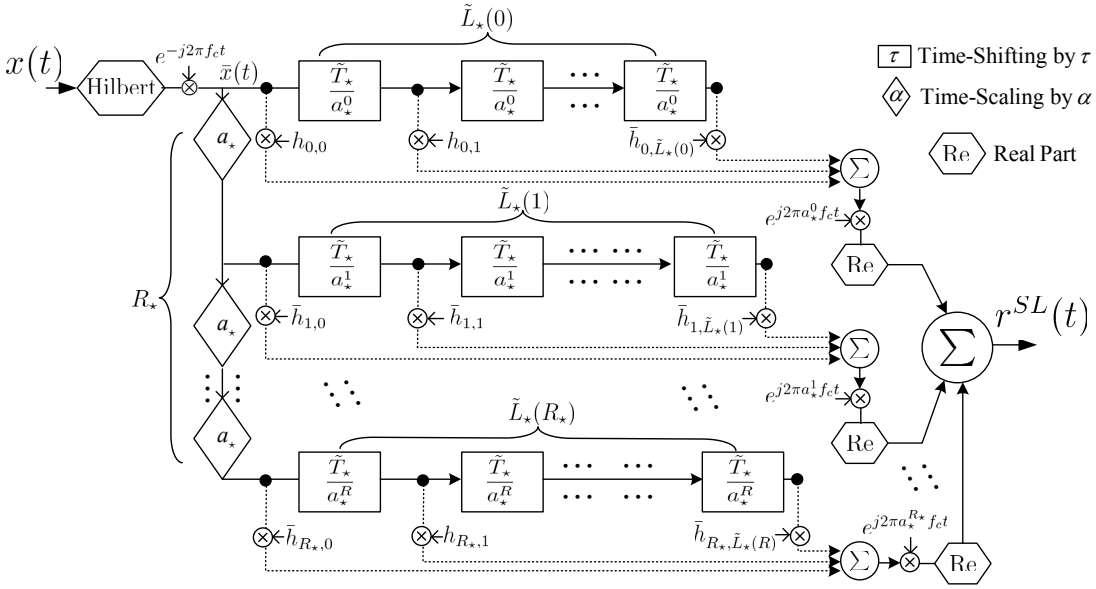

Fig. 2. Adaptation of the scale-lag canonical model to bandpass signals.

The other interesting thing about selecting $p(t)$ as in (13) is that $q_{r,l}(t) = \mathrm{sinc}(ta^r/\tilde{T} - l)$ and thus $\bar{g}_{r,n} = \bar{h}_{r,n}$, which results in the following simple discrete-time convolution input-output model:

$$\bar{y}_{r,n} = \sum_{l=0}^{\tilde{L}(r)} \bar{h}_{r,l} s_{n-l}. \tag{14}$$

V. Block Transmission

To aid block processing at the receiver, let us parse the information-carrying symbols b_n in blocks of length N, separated from each other by a cyclic prefix (CP) of length Z. For the first block of data, denoted as $\mathbf{b} = [b_0, \ldots, b_{N-1}]^T$, this means that the transmitted symbols s_n satisfy $s_n = b_{n-Z}$ for $Z \le n < N$ and $s_n = b_{N+n-Z}$ for $0 \le n < Z$. To avoid interblock interference (IBI) on every branch of the virtual MISO system, the CP length Z needs to satisfy $Z \ge \tilde{L}(r)$ for $r \in \{0, 1, \ldots, R\}$, or in other words, $Z \ge \lceil a^R \tau_{max}/\tilde{T} \rceil$. Removing the CP at the receiver, we can then obtain from (14) the following relationship for the first block of data of the rth branch of the virtual MISO system:

$$\bar{\mathbf{y}}_r = \bar{\mathbf{H}}_r \mathbf{b},$$

where $\bar{\mathbf{y}}_r = [\bar{y}_{r,Z}, \ldots, \bar{y}_{r,N+Z-1}]^T$ and $\bar{\mathbf{H}}_r$ is a circulant matrix with $[\bar{h}_{r,0}, \ldots, \bar{h}_{r,\tilde{L}(r)}, 0, \ldots, 0]^T$ as its first column. Collecting the outputs of all of the different branches of the virtual MISO system, yields

$$\bar{\mathbf{y}} = \bar{\mathbf{H}} \mathbf{b}, \tag{15}$$

where $\bar{\mathbf{y}} = [\bar{\mathbf{y}}_0^T, \ldots, \bar{\mathbf{y}}_R^T]^T$ and $\bar{\mathbf{H}} = [\bar{\mathbf{H}}_0^T, \ldots, \bar{\mathbf{H}}_R^T]^T$. Using discrete Fourier transform (DFT) processing and maximum ratio combining (MRC), $\mathbf{b}$ can then be easily recovered from $\bar{\mathbf{y}}$, even when noise is present.

Note that so far we have only discussed transmission on a single scale layer. In other words, we have limited ourselves to modulating symbols s_n on a single band of effective bandwidth $\tilde{W}_\star$ at carrier frequency f_c. But similar to [5], we could consider transmitting on multiple scale layers in parallel, and modulate symbols on K non-overlapping bands, where the kth band has bandwith $a^k \tilde{W}_\star$ and carrier frequency $a^k f_c$, with $k \in \{0, 1, \ldots, K-1\}$. Of course, in that case we obtain additional inter-scale interference and the model (15) changes into a linear relationship described by a block banded channel matrix. However, due to space limitations, we do not provide this extension herein.

VI. Computer Simulations

We first investigate the accuracy of the newly proposed model. More specifically, we assume that a single symbol $s_0 = 1$ is sent as described in Section IV, which means that $\bar{x}(t) = \tilde{W}_\star^{1/2} \mathrm{sinc}(\tilde{W}_\star t)$ and $x(t) = \tilde{W}_\star^{1/2} \cos(2\pi f_c t) \mathrm{sinc}(\tilde{W}_\star t)$. We then look at the normalized mean square error (NMSE) of the received signal, given by

$$\xi = \frac{\int_0^{\tau_{\max}} |r(t) - r^{\mathrm{SL}}(t)|^2 dt}{\int_0^{\tau_{\max}} |r(t)|^2}, \tag{16}$$

with $r^{\mathrm{SL}}(t)$ defined in (11). Different $\gamma = f_c/\tilde{W}_\star$ ratios are considered. For $\gamma = f_c/\tilde{W}_\star = 1.5$, we obtain a special case since then $x(t)$ is a Shannon wavelet with base time $T = 1/\tilde{W}_\star$ (which is not equal to $1/W_\star$!) and base scale $a = 2$, which also allows us to compute the MSE of the received signal as in (16) but using the $r^{\mathrm{SL}}(t)$ defined in (4).

Figure 3 shows the NMSE results for a channel with a uniform delay profile in the range $[0, 2/\tilde{W}_\star)$ and scales picked as $\alpha = 1.2^r$ for $r = 0, 1, 2, \ldots$. We clearly see that the adapted scale-lag canonical model (11) is more accurate than the former model (4). We especially observe a good fit when $\gamma = f_c/\tilde{W}_\star = 5.5$, which yields $a = 1.2$ according to (10), since in that case the actual scales $\alpha = 1.2^r$ match the scales a^r of the scale-lag canonical model.

Using the same channel model as before but fixing the $\alpha_{\max}$ to $\alpha_{\max} = 1.2$ (so the actual channel only has two scales), we now consider the block transmission scheme presented in Section V using $N = 16$ and $Z = 8$. Figure 4 shows the BER performance for different cases. As mentioned before, when $\gamma = f_c/\tilde{W}_\star = 5.5$, our channel model is more accurate and a much better performance is obtained.

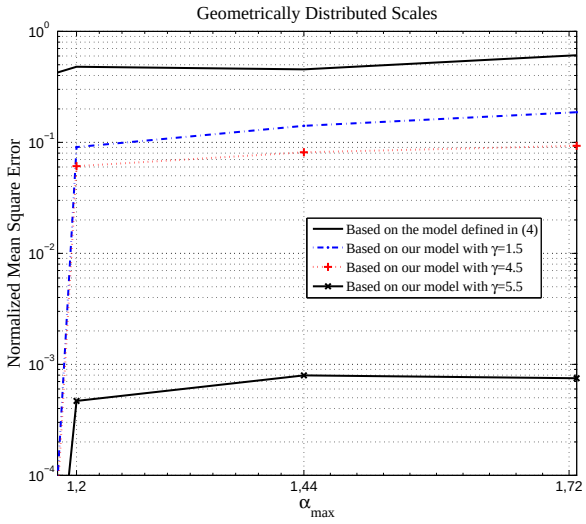

Fig. 3. NMSE of the different scale-lag canonical channel models.

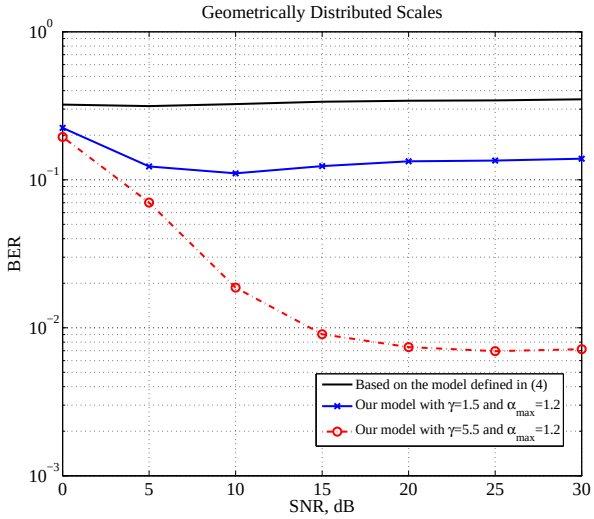

Fig. 4. BER performance for block transmission.

VII. Conclusions

In this paper, we have developed a new scale-lag canonical channel model for general multi-scale multi-lag wireless channels. The model is based on exploiting the bandpass nature of most communication signals, and solves some of the issues that were present in existing scale-lag canonical models. Furthermore, we developed a high-rate signaling scheme that fits this new channel model and leads to relatively simple receiver processing. The proposed channel model is validated by means of the MSE of the impulse response as well as the BER of the related communication scheme.

References

[1] A. M. Sayeed and B. Aazhang. Joint multipath-Doppler diversity in mobile wireless communications. *IEEE T. Commun.*, 47(1):123–132, 1999.

[2] S. Rickard, R. Balan, V. Poor, and S. Verdu. Canonical time-frequency, time-scale, and frequency-scale representations of time-varying channels. *J. Comm. Infor. Syst.*, 5(5):1–30, 2005.

[3] Y. Jiang and A. Papandreou-Suppappola. Discrete time-scale characterization of wideband time-varying systems. *IEEE T. Signal. Proces.*, 54(4):1364–1375, 2006.

[4] A. R. Margetts, P. Schniter, and A. Swami. Joint scale-lag diversity in wideband mobile direct sequence spread spectrum systems. *IEEE T. Wirel. Commun.*, 6(12):4308–4319, 2007.

[5] T. Xu, G. Leus, and U. Mitra. Othogonal wavelet division multiplexing for wideband time-varying channels. submitted to ICASSP 2011.

[6] B. Li, S. Zhou, M. Stojanovic, L. Freitag, and P. Willett. Multicarrier communication over underwater acoustic channels with nonuniform doppler shifts. *IEEE J. Oceanic. Eng.*, 33(2):198–209, 2008.

[7] A.-B. Salberg and A. Swami. Doppler and frequency-offset synchronization in wideband OFDM. *IEEE T. Wirel. Commun.*, 4(6):2870–2881, 2005.

[8] P. A. van Walree and G. Leus. Robust underwater telemetry with adaptive turbo multiband equalization. *IEEE J. Oceanic. Eng.*, 34(4):645–655, 2009.

[9] M. K. Tsatsanis and G. B. Giannakis. Time-varying system identification and model validation using wavelets. *IEEE T. Signal. Proces.*, 41(12):3512–3523, 1993.

[10] M. I. Doroslovacki and H. Fan. Wavelet-based linear system modeling and adaptive filtering. *IEEE T. Signal. Proces.*, 44(5):1156–1167, 1996.

[11] M. Martone. Wavelet-based separating kernels for array processing of cellular DS/CDMA signals in fast fading. *IEEE T. Commun.*, 48(6):979–995, 2000.

[12] L. H. Sibul, L.G. Weiss, and T.L. Dixon. Characterization of stochastic propagation and scattering via gabor and wavelet transforms. *Journal of Computational Acoustics*, 2(1):345–369, Jan. 1994.